Journal of Statistical Physics, Vol. 53, Nos. 5/6, 1988

Finite-Size Corrections for Inclined Interfaces in Two Dimensions: Exact Results for Ising and Solid-on-Solid Models

N. M. Švrakić,[1] V. Privman,[1] and D. B. Abraham[2]

Received May 26, 1988; revision received July 19, 1988

Analysis of finite-size corrections for the surface tension and surface stiffness coefficients in two-dimensional models with inclined interfaces is presented. We obtain a universal leading contribution proportional to $(\ln L)/L$ for the 2D system of size L. By explicit calculations for restricted and unrestricted solid-on-solid models and the square lattice Ising model, we demonstrate the Gaussian nature of rough interfaces with fixed ends, and derive the leading $1/L$-type corrections for appropriate surface quantities.

KEY WORDS: Finite-size properties; Ising models; surface tension; solid-on-solid approximation.

1. INTRODUCTION

When thermodynamic system fluctuations are on a scale comparable to sample dimensions, the effects of finite size begin to play a major role. Studies of such finite-size effects, and of finite-size scaling in general, are of great importance for the theory of critical phenomena and for the interpretation of experimental and Monte Carlo data. When the finite-size corrections are known, the infinite-system (thermodynamic-limit) quantities can then be estimated by the use of proper extrapolation procedures.

Finite-size scaling theory for the first- and second-order *bulk* phase transitions has been extensively developed in recent years (see refs. 1–6 for reviews). In addition, several results are available in the active field of *surface* and *interface* phase transitions.[7] Specifically, mean field methods[8]

[1] Department of Physics, Clarkson University, Potsdam, New York 13676.
[2] Department of Mathematics, University of Arizona, Tucson, Arizona 85721.

0022-4715/88/1200-1041$06.00/0

and exact calculations for the two-dimensional (2D) Ising model[9–11] have been used to assess the effect of surfaces and interfaces on the bulk scaling behavior. Finite-size scaling at first-order *wetting* transitions has been studied recently[12] for the 2D Ising model; the second-order wetting transition was analyzed for the 2D solid-on-solid (SOS) model.[13] Furthermore, mean field results were obtained[14] for the size effects on the thickness of wetting layers. Finally, universal scaling forms of the correlation length were reported[15] for Ising strips with various boundary conditions.

In studies of interfacial properties of lattice models, the average orientation of the interface is usually taken to be along one of the principal axes of the system. However, recent Monte Carlo studies[16] of the roughening transition and related interfacial properties of the 3D Ising model have raised an important theoretical question regarding the finite-size effects on the *anisotropic* (angle-dependent) surface tension of rough interfaces. This issue has been addressed in refs. 17 and 18. Finite-size corrections for rough interfaces, i.e., for temperatures $T_R < T < T_c$ in three dimensions and $0 < T < T_c$ in two dimensions, were derived and a universal leading contribution proportional to $(\ln L)/L$ was predicted for the 2D systems of size L. These results are based on the well-established directed random walk-like (Gaussian) properties of line interfaces in two dimensions.[19] Corresponding results for 3D systems have also been derived and justified by phenomenological arguments.[17] Recently, Gelfand and Fisher have developed[18] a theory of finite-size effects on surface tension for general dimension, within the capillary wave type approach.[20,21] Whenever comparison is possible, the results of various approaches are consistent.

In this work we present explicit calculations of finite-size corrections for the surface tension and surface stiffness coefficient in two-dimensional SOS and Ising models. Our purpose is to provide a "microscopic" derivation of finite-size corrections and compare them with those predicted in refs. 17 and 18. Our results fully confirm the phenomenological theory.[17]

The format of this paper is as follows. In Section 2, we define the 2D Ising and SOS models with inclined interfaces and summarize predictions of the finite-size scaling theory for such interfaces. In Section 3, the leading-order results for the Ising and SOS models are derived and the Gaussian nature of interfacial properties is explicitly verified. Some of these results are implicit in the earlier work of Park *et al.*[22] for the SOS model and of Abraham[23] for the Ising model. Section 4 describes in detail the derivation of $1/L$-type finite-size corrections for the surface tension and stiffness coefficient of inclined interfaces in SOS and Ising models. Our results are briefly summarized in Section 5, which is also devoted to discussion and conclusions. Appendix A presents further exact calculation of the SOS

model partition functions, while Appendix B is devoted to the discussion of the low-temperature regime in which the various SOS and Ising model results become identical.

2. ISING INTERFACE IN TWO DIMENSIONS: DEFINITION OF THE MODEL

Consider a planar lattice of Ising spins $s(x, y) = \pm 1$ located at lattice points (x, y), with $x = 0, 1, 2, \ldots, L$, and $y = \pm\frac{1}{2}, \pm\frac{3}{2}, \ldots, \pm(M - \frac{1}{2})$, as shown in Fig. 1. The spins interact via nearest-neighbor ferromagnetic interactions J_x and J_y, with $J_{x,y} > 0$. The corresponding configurational energy, scaled by $k_B T$, is given by

$$E = -K_y \sum_{x=0}^{L} \sum_{y=-(M-1/2)}^{(M-3/2)} s(x, y)\, s(x, y+1) - K_x \sum_{x=0}^{L-1} \sum_{y=-(M-1/2)}^{(M-1/2)} s(x, y)\, s(x+1, y) \tag{2.1}$$

where $K_{x,y} = J_{x,y}/k_B T$.

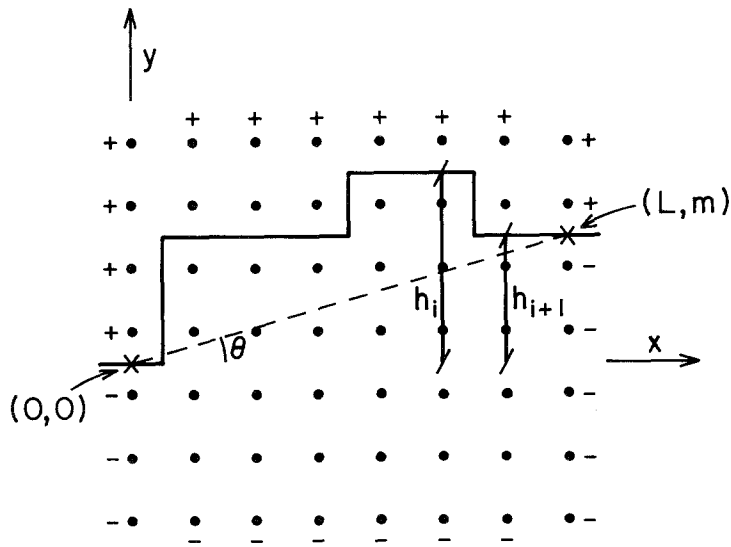

Fig. 1. Two-dimensional Ising model with inclined interface pinned by its endpoints (0, 0) and (L, m). The average inclination angle is specified by $\tan\theta = m/L$. The solid-on-solid configuration of the interface is shown by the solid line and is uniquely specified by the height variables h_i.

In what follows we will make use of two types of boundary conditions:

$$\mathscr{A}: \quad s(x, \pm(M-\tfrac{1}{2})) = +1, \qquad s(0, y) = s(L, y) = +1 \tag{2.2}$$

which, for $T < T_c$, select states with positive spontaneous magnetization, and

$$\mathscr{B}: \quad s(x, \pm(M-\tfrac{1}{2})) = \pm 1, \quad s(0, y \gtrless 0) = \pm 1, \quad s(L, y \gtrless m) = \pm 1 \tag{2.3}$$

which force a *long contour*, beginning at $(0, 0)$ and ending at (L, m), which separates the region of negative spontaneous magnetization from the region of positive spontaneous magnetization (see Fig. 1). Note that the average inclination of the interface can be measured by the angle θ given by $\tan\theta = m/L$. Thus, an Ising system of size $2(M-1) \times L$ with an interface forming an average angle θ with the x axis is considered. This interface can have arbitrary configurations consistent with the boundary conditions $\mathscr{B}$. The partition function for the Ising model defined above can be obtained along the lines of refs. 9–11 and 23. We will describe this calculation in Section 3.

The subset of *solid-on-solid* (SOS) interface configurations is selected by the requirement that there are no overhangs and bubbles (islands). Such configurations are then uniquely specified by the set of interface heights h_i, measured from the reference level $y = 0$, as shown in Fig. 1. Obviously, the heights can take values

$$h_i = 0, \pm 1, \pm 2, \ldots, \pm(M-1) \qquad \text{for} \quad i = 1, 2, \ldots, L-1 \tag{2.4}$$

In order to satisfy boundary conditions $\mathscr{B}$, we require that

$$h_0 = 0 \qquad \text{and} \qquad h_L = m \tag{2.5}$$

i.e., the interface is pinned by its endpoints at $(0, 0)$ and (L, m). A typical SOS configuration of the long contour is shown in Fig. 1. The corresponding SOS interfacial Hamiltonian, scaled by $k_B T$, is

$$H_{\mathrm{SOS}} = U \sum_{i=1}^{L-1} |h_{i+1} - h_i| + (L+1)\, V \tag{2.6}$$

The first term in this expression, with $U > 0$, mimics the surface tension contribution; it has the smallest value when all the heights h_i are equal. The second term is obtained by counting the number of times the interface cuts across the vertical bonds (each time a contribution V is added). For the SOS configurations (no overhangs or islands) the number of such crossings

is always equal to $L+1$. The SOS model partition function $Z(m, L; M)$ is calculated from

$$Z_{\mathrm{SOS}}(m, L; M) = \sum_{\{h_i\}} \exp(-H_{\mathrm{SOS}}) \tag{2.7}$$

with (2.4) and (2.5), and the summation in (2.7) is over all allowed configurations $\{h_i\}$ of the interface.

We will also consider the *restricted solid-on-solid* (RSOS) model, which is obtained when the height differences in (2.6) are restricted to

$$|h_{i+1} - h_i| = 0, 1 \qquad \text{for all} \quad i \tag{2.8}$$

The critical behavior of the RSOS model is the same as that of the SOS model; however, the former is often considered for mathematical convenience. In the following, we will analyze all three models (SOS, RSOS, and Ising) and calculate finite-size corrections approximately (Section 3) and exactly (Section 4). Presently, let us sumarize the finite-size properties of interfaces in 2D systems, as predicted by the general theory of ref. 17.

Let $Z(m, L; M) = \mathscr{Z}_{\mathscr{B}}/\mathscr{Z}_{\mathscr{A}}$, with the boundary conditions $\mathscr{A}$ and $\mathscr{B}$ defined in (2.2) and (2.3), denote the normalized partition function of an Ising-like system. For *fixed* m, with L and M large, the step free energy in two dimensions is defined[17] by

$$s(m, L; M) = -\ln \frac{Z(m, L; M)}{Z(0, L; M)} \tag{2.9}$$

in units of $k_{\mathrm{B}}T$. If the inclination angle θ is fixed by the requirement that $m = L \tan\theta$ (see Fig. 1), the surface tension per unit length, in units of $k_{\mathrm{B}}T$, can be obtained from

$$\sigma(\theta, L; M) = -\frac{\cos\theta}{L} \ln Z(L \tan\theta, L; M) \tag{2.10}$$

For the geometry of Fig. 1, when the x axis coincides with the symmetry direction of the lattice, and with the assumption of the local minimum[17] of $\sigma(\theta)/\cos\theta$, the corresponding *bulk* ($L = M = \infty$) quantities are

$$s(m, \infty, \infty) = 0 \tag{2.11}$$

and

$$\frac{\sigma(\theta, \infty, \infty)}{\cos\theta} = \tau + \frac{1}{2}\kappa\theta^2 + O(\theta^4) \tag{2.12}$$

where

$$\tau \equiv \sigma(0, \infty, \infty) > 0, \qquad \kappa \equiv \sigma(0, \infty, \infty) + \sigma''(0, \infty, \infty) > 0 \tag{2.13}$$

We will always assume that $M = O(L)$ and $|m| \ll L$, which corresponds to $|\theta| \ll 1$ in (2.10). The quantity κ introduced in (2.12) is the surface

stiffness coefficient.[17] In order to obtain the finite-size corrections for quantities τ and κ in (2.12) and (2.13), we recall that the linear interface of length L fluctuates in the transverse direction on the scale $\sim\sqrt{L}$. Therefore, when the size of the system in the transverse direction (M) is of order $\sqrt{L}$ or smaller, the interface fluctuations will be suppressed. However, since we assume $M = O(L)$, the finite-M effects are exponentially small in $M^2/L \sim L$ and can be omitted. (In the next sections a mathematically precise verification of these statements will be given.) We are therefore left with the problem of determining finite-L, power-law corrections to the surface tension and stiffness. (Terms which are exponentially small in L will be neglected.) Such corrections have been estimated[17] by the following argument. Consider a long contour, with its endpoints pinned at (0, 0) and (L, m), as depicted in Fig. 1. The SOS configurations of this contour can be brought into a one-to-one correspondence[10,19] with directed random walks between the same endpoints. The probability distribution for such a walk, starting from the origin, to reach the point (L, m), with $m = L \tan\theta \sim L\theta$, is Gaussian in m, for $m \ll L$, with width $\sim\sqrt{L}$.

This directed random walk-like property of line interfaces in two dimensions is rather general.[19] Therefore, the following general phenomenological expression for the partition function has been proposed[17]:

$$Z(m, L) \simeq \exp(-\tau_L L)\left(\frac{\kappa_L}{2\pi L}\right)^{1/2} \exp\left(\frac{-\kappa_L m^2}{2L}\right) \tag{2.14}$$

Note that the original formula in ref. 17 [Eq. (5)] contains in addition the lattice spacing, denoted by λ there, which is assumed to be unity throughout this paper. (Lattice spacing is one of the natural lengths in the problem and must be taken into account in order to properly scale other units of length.) The first term in (2.14) determines the free energy cost of creating an interface of length L. We thus expect that $\lim_{L\to\infty} \tau_L = \tau$. The last term, Gaussian in m (or θ), represents additional entropic effects due to the interface inclination, measured with respect to $\theta = 0$. The surface stiffness coefficient κ in the bulk limit is given by (2.13), so that we expect $\lim_{L\to\infty} \kappa_L = \kappa$. Finally, the square root term in (2.14) comes from the normalization of the Gaussian distribution.[17]

Assuming that τ_L and κ_L are noncritical, the standard $O(1/L)$ "endpoint" finite-size corrections for these quantities have been conjectured.[17] Specifically,

$$\tau_L = \tau + \frac{a}{L} + o\left(\frac{1}{L}\right), \qquad \kappa_L = \kappa + \frac{b}{L} + o\left(\frac{1}{L}\right) \tag{2.15}$$

where a, b, and other "constants" are temperature dependent. Using (2.14) and (2.15), with definitions (2.10) and (2.13), the following finite-size relations are easily derived:

$$\sigma(0, L) = \sigma(0, \infty) + \frac{\ln L}{2L} + \frac{a - \ln[(\kappa/2\pi)^{1/2}]}{L} + o\left(\frac{1}{L}\right) \tag{2.16}$$

$$\sigma''(0, L) = \sigma''(0, \infty) - \frac{\ln L}{2L} + \frac{b - a + \ln[(\kappa/2\pi)^{1/2}]}{L} + o\left(\frac{1}{L}\right) \tag{2.17}$$

Note that the leading correction terms $\pm(\ln L)/2L$ have no free parameters.

The step free energy $s(m, L)$ is now readily obtained from (2.9) and (2.14). We get

$$s(m, L) \simeq \kappa m^2/2L \tag{2.18}$$

A result equivalent to (2.18) was derived earlier by Fisher and Weeks[20] within the capillary-wave theory. The argument similar to the one leading to (2.18) has been extended[17,18,20] to 3D systems with $T > T_R$, i.e., for rough interfaces. We consider in this work the 2D case only, so that $T_R = 0$. In the next section we derive the Gaussian form (2.14) by explicit model calculations.

3. GAUSSIAN BEHAVIOR OF LINE INTERFACES

In this section we set up the problem of calculating the partition function for a system with an inclined interface and show that, to leading order, it has the conjectured Gaussian form (2.14). The calculation will be performed for both unrestricted and restricted solid-on-solid models. We then outline Ising model results of a similar nature.

In order to calculate the partition function (2.7), we will use the transfer matrix technique. First, introduce the variables

$$u = \exp(-U), \qquad v = \exp(-V) \tag{3.1}$$

and define a transfer matrix T with elements

$$T_{nj}^{\mathrm{SOS}} = u^{|n-j|}, \qquad T_{nj}^{\mathrm{RSOS}} = u^{|n-j|}(\delta_{0,n-j} + \delta_{1,|n-j|}) \tag{3.2}$$

for the SOS and RSOS models, respectively. The partition function is then expressed as

$$Z_{\mathrm{SOS}}(m, L; M) = v^{L+1} \langle 0 \,|T^L|\, m \rangle \tag{3.3}$$

where the states $\langle 0|$ and $|m\rangle$ correspond to vectors of length $2M-1$ with the single nonzero entry $g_0=1$ or $g_m=1$. These vectors correspond to the boundary conditions $\mathscr{B}$. Expression (3.3) is evaluated, as usual, by calculating the eigenvalues and eigenvectors of T. Let us, for simplicity, consider first the RSOS model. In this case $T_{nj}=0$ except for $|n-j|=0, 1$ [see (2.8)] and the matrix T is tridiagonal. The eigenequation is

$$\sum_j T_{nj} g_j = \lambda g_n \tag{3.4}$$

where the g_i are the eigenvector elements and λ is the eigenvalue. These equations reduce to

$$u g_{n+1} + g_n + u g_{n-1} = \lambda g_n \qquad \text{for} \quad -(M-2) \leqslant n \leqslant M-2 \tag{3.5}$$

and the boundary conditions

$$\begin{aligned} g_{M-1} + u g_{M-2} &= \lambda g_{M-1} \\ g_{1-M} + u g_{2-M} &= \lambda g_{1-M} \end{aligned} \tag{3.6}$$

It is easy to see that (3.5) has solutions which can be even or odd in n. However, the odd solutions are orthogonal to the vector $\langle 0|$ appearing in (3.3) and do not contribute to the partition function. We therefore seek solutions of (3.5) in the form

$$g_n = C \cos nq \tag{3.7}$$

where $C=1/\sqrt{M}$ is the normalization constant. Solution (3.7) will satisfy the recurrence (3.5) provided

$$\lambda(q) = 1 + 2u \cos q \tag{3.8}$$

Finally, substituting (3.7) in the boundary conditions (3.6), we obtain the quantization condition for q, i.e., $\cos Mq = 0$, or

$$q_j = \frac{(2j+1)\,\pi}{2M}, \qquad j=0, 1, \ldots, M-1 \tag{3.9}$$

The RSOS model transfer matrix therefore has M "even" eigenvalues $\lambda_j \equiv \lambda(q_j)$, where q_j and $\lambda(q_j)$ are given by (3.9) and (3.8), respectively.

The eigenproblem for the unrestricted SOS model can be solved in a similar way by using the fact that the *inverse* of T is a tridiagonal matrix. The symmetric eigenvector elements are also given by (3.7). We note that, in the case of the unrestricted SOS model, the quantization condition, yielding M even eigenvalues, is

$$\cot Mq = \frac{u \sin q}{1 - u \cos q} \tag{3.10}$$

in place of (3.9). Thus, the q_j are not equally spaced and depend on u. For sufficiently large M, the solutions of (3.10) approach (3.9) with an error of the order $1/M^2$. Finally, the eigenvalues of the unrestricted SOS model transfer matrix are given by

$$\lambda(q) = \frac{1-u^2}{1-2u\cos q + u^2} \tag{3.11}$$

instead of (3.8).

The partition function $Z(m, L; M)$ for the RSOS model is obtained from (3.3). The right-hand side of (3.3) can be written in a more convenient form if the complete set of orthonormal states $|q_j\rangle$ is inserted. We obtain

$$Z(m, L; M) = v^{L+1} \sum_{\{q_j\}} \langle 0|q_j\rangle \lambda_j^L \langle q_j|m\rangle \tag{3.12}$$

By using the explicit expression (3.7) for $|q_j\rangle$ and the fact that for the RSOS model

$$q_{j+1} - q_j = \pi/M \tag{3.13}$$

[see (3.9)], Eq. (3.12) can be further expressed as

$$Z(m, L; M) = \frac{v^{L+1}}{\pi} \sum_{j=0}^{M-1} (q_{j+1} - q_j)\, \lambda_j^L \cos mq_j \tag{3.14}$$

for the RSOS model. For $M \to \infty$ this sum converges to an integral

$$Z(m, L; \infty) \equiv Z(m, L) = \frac{v^{L+1}}{2\pi} \int_{-\pi}^{\pi} \lambda^L(q) \cos mq\, dq \tag{3.15}$$

with an error exponentially small in M^2/L. Specifically, the leading difference between (3.14) and (3.15) for the RSOS model is of the form

$$\frac{Z(m, L; \infty) - Z(m, L; M)}{Z(m, L; \infty)} \simeq 2 \exp\left(-\frac{(1+2u)\, M^2}{uL}\right) \cosh \frac{(1+2u)\, Mm}{uL} \tag{3.16}$$

Therefore, as long as $M \geqslant \sqrt{L}$, the finite-M effects can be neglected. This provides mathematical justification for neglecting such effects in this paper, since we are assuming that $M = O(L)$ [see discussion following (2.13)].

For the SOS model, the transition from a sum of the type (3.12) to an integral form similar to (3.15) is more complicated. This is due to the fact that the q_j in this case are not equally spaced and relation (3.13) is not strictly satisfied, i.e., this relation has additional terms of order $1/M^2$. Thus,

while it is obvious that the sum (3.12) for the SOS model converges to the integral (3.15) with (3.11), the precise form of this convergence, i.e., a relation analogous to (3.16), is more difficult to obtain. We have not investigated this matter in detail since this would lead to unilluminating mathematical complications.

The $M=\infty$ partition functions for the specific models are thus given by

$$Z_{\mathrm{RSOS}}(m, L)=\frac{v^{L+1}}{2\pi}\int_{-\pi}^{\pi}(1+2u\cos q)^{L}\cos mq\,dq \tag{3.17}$$

and

$$Z_{\mathrm{SOS}}(m, L)=\frac{v^{L+1}(1-u^{2})^{L}}{2\pi}\int_{-\pi}^{\pi}\frac{\cos mq\,dq}{(1-2u\cos q+u^{2})^{L}} \tag{3.18}$$

These functions can be calculated exactly by analytic evaluation of the integrals. We describe these calculations in Appendix A. For the purposes of the present section, however, in order to show that the leading behavior of $Z(m, L)$ is Gaussian in m, i.e., of the form (2.14), it is sufficient to evaluate the integrals in (3.17) and (3.18) approximately. In particular, let us replace $\cos q\simeq 1-q^{2}/2$, and further put $(1\pm\mathrm{const}\cdot q^{2})^{L}\simeq \exp(\pm\mathrm{const}\cdot q^{2}L)$. This leads to the following expressions:

$$Z_{\mathrm{RSOS}}(m, L)\simeq\frac{v^{L+1}(1+2u)^{L}}{2\pi}\int_{-\pi}^{\pi}\exp\left(-\frac{uLq^{2}}{1+2u}\right)\cos mq\,dq \tag{3.19}$$

$$Z_{\mathrm{SOS}}(m, L)\simeq\frac{v^{L+1}}{2\pi}\left(\frac{1+u}{1-u}\right)^{L}\int_{-\pi}^{\pi}\exp\left(-\frac{uLq^{2}}{(1-u)^{2}}\right)\cos mq\,dq \tag{3.20}$$

Observe that the integrals are saturated at $|q|\leqslant 1/\sqrt{L}$, which justifies the small-q approximation. Finally, since L is large, the limits of integration in (3.19) and (3.20) can be extended to $(-\infty, +\infty)$. Thus, we obtain

$$Z_{\mathrm{RSOS}}(m, L)\simeq v^{L+1}(1+2u)^{L}\left(\frac{1+2u}{2u}\frac{1}{2\pi L}\right)^{1/2}\times\exp\left(-\frac{m^{2}}{2L}\frac{1+2u}{2u}\right) \tag{3.21}$$

and

$$Z_{\mathrm{SOS}}(m, L)\simeq v^{L+1}\left(\frac{1+u}{1-u}\right)^{L}\left[\frac{(1-u)^{2}}{2u}\frac{1}{2\pi L}\right]^{1/2}\times\exp\left[-\frac{m^{2}}{2L}\frac{(1-u)^{2}}{2u}\right] \tag{3.22}$$

Expressions (3.21) and (3.22) are precisely of the Gaussian form (2.14). The above is therefore a "microscopic" derivation of random walk-like property of line interfaces. As mentioned in the Introduction, the result (3.22) is implicit in ref. 22. In the next section, we will show *a posteriori*, by a systematic expansion of the partition functions (3.17) and (3.18), that the approximations (3.21)–(3.22) are indeed valid, and calculate the leading corrections.

By comparing (3.21) and (3.22) with (2.14), the bulk values for τ and κ [see (2.15)] can be simply read off. They are

$$\tau = -\ln[v(1+2u)], \qquad \kappa = \frac{1+2u}{2u} \qquad \text{(RSOS model)} \tag{3.23}$$

and

$$\tau = -\ln\left[v\left(\frac{1+u}{1-u}\right)\right], \qquad \kappa = \frac{(1-u)^2}{2u} \qquad \text{(SOS model)} \tag{3.24}$$

Note that the above expressions for the two models become equivalent for small u, i.e., at low temperatures, as expected.

Approximate expressions similar to (3.21) and (3.22) can also be derived the Ising model specified by (2.1). Using the well-known duality relation[10,11,23] between the correlation function and the interfacial free energy, the partition function for the Ising model can be obtained in the form

$$Z_{\text{Ising}}(m, L) = \frac{e^{-2K_y}}{2\pi} \int_{-\pi}^{\pi} \frac{\cos mq \, dq}{\cosh L\gamma(q) + \sinh L\gamma(q) \cos \delta^*(q)} \tag{3.25}$$

Here $\gamma(q)$ and $\delta^*(q)$ are the elements of Onsager's hyperbolic triangle[23]

$$\cosh \gamma(q) = \cosh 2K_x^* \cosh 2K_y - \sinh 2K_x^* \sinh 2K_y \cos q \tag{3.26}$$

$$\cos \delta^*(q) = \frac{\cosh 2K_y \cosh \gamma(q) - \cosh 2K_x^*}{\sinh 2K_y \sinh \gamma(q)} \tag{3.27}$$

and the dual couplings $K_{x,y}^*$ are defined by $\exp(-2K_{x,y}) = \tanh K_{x,y}^*$. In (3.26) we select the branch for which $\gamma(q) > 0$. (Recall that $T < T_c$ here.) Note that the partition function (3.25) has the same structure as the analogous SOS and RSOS partiton functions (3.17) and (3.18). In particular, by neglecting terms exponentially small in L, we can write (3.25) in the form

$$Z_{\text{Ising}}(m, L) \simeq \frac{\exp(-2K_y)}{2\pi} \int_{-\pi}^{\pi} \frac{2 \exp[-L\gamma(q)] \cos mq \, dq}{1 + \cos \delta^*(q)} \tag{3.28}$$

The functions $\gamma(q)$ and $\cos\delta^*(q)$ in this expression can be expanded for small q, yielding the exponential factor with the leading q dependence of the form $\exp(\text{const}\cdot q^2 L)$. The integration, when extended to the interval $(-\infty, +\infty)$, can then be performed easily. We get (up to a constant prefactor)

$$Z_{\text{Ising}}(m, L) \sim \exp[-L\gamma(0)] \left[\frac{\sinh\gamma(0)}{\sinh 2K_x^* \sinh 2K_y} \frac{1}{2\pi L} \right]^{1/2} \times \exp\left[-\frac{m^2 \sinh\gamma(0)}{2L \sinh 2K_x^* \sinh 2K_y} \right] \tag{3.29}$$

where we used

$$\gamma(q) = \gamma(0) + \frac{q^2}{2} \frac{\sinh 2K_x^* \sinh 2K_y}{\sinh\gamma(0)} + O(q^4), \quad \cos\delta^*(q) = 1 + O(q^2) \tag{3.30}$$

Clearly, the partition function (3.29) has the Gaussian form (2.14), as conjectured.[17] We thus obtain the well-known results for the Ising model

$$\tau = \gamma(0), \qquad \kappa = \frac{\sinh\gamma(0)}{\sinh 2K_x^* \sinh 2K_y} \tag{3.31}$$

by comparing (3.29) with (2.14) and (2.15). Recall[10] that $\gamma(0)$ is precisely equal to the bulk surface tension of the Ising model: $\gamma(0) = 2(K_y - K_x^*)$. The relations (3.29) and (3.30) simplify for the isotropic model, i.e., when $K_x = K_y \equiv K$, since $\sinh 2K^* \sinh 2K = 1$. In the next section, the leading finite-size corrections to τ and κ for all three models (SOS, RSOS, and Ising) will be calculated.

4. FINITE-SIZE PROPERTIES OF INCLINED INTERFACES: EXACT RESULTS FOR ISING AND SOS MODELS

In this section we derive exact expressions for the surface tension and stiffness coefficient of the inclined interface shown in Fig. 1. As in Section 3, we will assume that $M \sim O(L)$, so that the partition functions $Z_{\text{SOS}}(m, L)$, $Z_{\text{RSOS}}(m, L)$, and $Z_{\text{Ising}}(m, L)$ are given by (3.17), (3.18), and (3.28), with corrections exponentially small in M^2/L, as discussed earlier. We consider first the SOS models.

It turns out that the integrals in (3.17) and (3.18) can be evaluated analytically in terms of the hypergeometric functions ${}_2F_1$. These calculation are described in Appendix A. However, the expressions thus obtained are not very useful for finite-size analyses. Instead, in order to obtain $Z(m, L)$

as asymptotic series in powers of $1/L$, we evaluate the integrals (3.17) and (3.18) [and later (3.25)] for large L by a steepest-descent-type method. In particular, the integrals (3.17) and (3.18) can be more conveniently written as

$$Z(m, L) = \frac{v^{L+1}}{2\pi} \int_{-\pi}^{\pi} \exp\{L[\ln \lambda(q) + iq \tan \theta]\}\, dq \tag{4.1}$$

where $\lambda(q)$ is given by (3.11) [(3.8)] for the SOS [RSOS] model, and we used $m = L \tan \theta$. Similar expression can also be derived for the Ising model (see below). An integral of the type (4.1) has to be analyzed for large L. Let us consider the SOS model in some detail. In this case, (4.1) becomes

$$Z_{\mathrm{SOS}}(m, L) = \frac{v^{L+1}(1-u^2)^L}{2\pi} \times \int_{-\pi}^{\pi} \exp\{-L[\ln(1 - 2u \cos q + u^2) - iq \tan \theta]\}\, dq \tag{4.2}$$

To proceed, we expand the function

$$f(q) = \ln(1 - 2u \cos q + u^2) - iq \tan \theta \tag{4.3}$$

near the extremum at q_0 given by

$$q_0 = i \sinh^{-1}\left(\frac{\tan 2\theta}{2}\left\{\frac{1+u^2}{2u} - \left[1 + \frac{(1-u^2)^2 \tan^2 \theta}{4u^2}\right]^{1/2}\right\}\right) \tag{4.4}$$

which, for small θ, has the form

$$q_0 = i \frac{(1-u)^2 \tan \theta}{2u}\left[1 + O(\tan^2 \theta)\right] \tag{4.5}$$

The function $f(q)$ is expanded as

$$f(q) = f(q_0) + \frac{1}{2!} f''(q_0)(q - q_0)^2 + \cdots \tag{4.6}$$

where

$$f(q_0) = 2 \ln(1-u) + \frac{\tan^2 \theta}{2} \frac{(1-u)^2}{2u} + O(\tan^4 \theta) \tag{4.7}$$

and

$$f''(q_0) = \frac{2u}{(1-u)^2}\left[1 + \tan^2 \theta \frac{(1-u)^2 (1 + 4u + u^2)}{8u^2} + O(\tan^4 \theta)\right] \tag{4.8}$$

Substituting (4.6)–(4.8) in the integral (4.2), shifting the contour, extending the limits of integration to $(-\infty, +\infty)$, etc., we finally obtain

$$Z_{\mathrm{SOS}}(\tan\theta, L) \simeq v^{L+1}\left(\frac{1+u}{1-u}\right)^{L}\left[\frac{(1-u)^2}{2u}\frac{1}{2\pi L}\right]^{1/2} \times \exp\left\{-L\frac{\tan^2\theta}{2}\left[\frac{(1-u)^2}{2u}+\frac{(1-u)^2(1+4u+u^2)}{8u^2L}+O\left(\frac{1}{L^2}\right)\right]\right\} \tag{4.9}$$

In order to obtain finite-L corrections for the surface stiffness coefficient κ_L [see (2.15)], we form the ratio

$$\frac{Z_{\mathrm{SOS}}(\theta, L)}{Z_{\mathrm{SOS}}(0, L)} = \exp\left(-L\frac{\theta^2\kappa_L}{2}\right) \tag{4.10}$$

[see (2.14)], from which, by the use of (4.9), we obtain the leading finite-L behavior of κ_L in the form (2.15), with

$$\kappa = \frac{(1-u)^2}{2u}, \qquad b = \frac{(1-u)^2(1+4u+u^2)}{8u^2} \qquad \text{(SOS model)} \tag{4.11}$$

Similarly, by comparing $Z_{\mathrm{SOS}}(0, L)$ from (4.9) with (2.14), we find that the leading large-L behavior of τ_L is of the form (2.15) with

$$\tau = -\ln\left[v\left(\frac{1+u}{1-u}\right)\right], \qquad a = -\ln v \qquad \text{(SOS model)} \tag{4.12}$$

Corresponding calculations for the RSOS model are almost identical with the above, and we only quote the results here. The surface tension and the surface stiffness coefficient are again of the form (2.15)–(2.17) with

$$\tau = -\ln[v(1+2u)], \qquad a = -\ln v \tag{4.13}$$

$$\kappa = \frac{1+2u}{2u}, \qquad b = \frac{1-2u-8u^2}{8u^2} \qquad \text{(RSOS model)} \tag{4.14}$$

Note that b changes sign at $u = 1/4$.

The Ising model calculation can also be performed along the same lines starting from the expression (3.28). In this case there is a slight complication due to the term $[1+\cos\delta^*(q)]$ in the denominator of the integrand [see (3.28)]. However, this function can be expanded in powers of $(q-q_0)$ and integrated term by term. It is easy to see that the first non-

trivial contribution of this factor to the finite-L corrections will be of order $1/L$ for the surface stiffness coefficient and of order $1/L^2$ for the surface tension. The remaining calculations are straightforward but cumbersome. We only quote the $K_x = K_y = K$ results here (see Appendix B for $K_x \neq K_y$). The surface tension τ_L and stiffness coefficient κ_L are of the form (2.15)–(2.17) with

$$\tau = \gamma(0), \qquad a = 2K \tag{4.15}$$

and

$$\kappa = \sinh \gamma(0), \qquad b = \tfrac{1}{2}[\sinh^2 2K^* + \sinh^2 \gamma(0) + 3 \cosh \gamma(0)] \tag{4.16}$$

for the Ising model.

5. SUMMARY AND CONCLUSIONS

In summary, we have shown by explicit calculations for the SOS, RSOS, and Ising models with inclined interfaces that the leading finite-size behavior is precisely as predicted by the finite-size scaling theory of ref. 17. We have demonstrated the Gaussian, or random walk, property of line interfaces in these models. Note that the $1/\sqrt{L}$ prefactor in the partition function (2.14) may not be strictly associated with the Gaussian form but may also be present in a more general m dependence, as detailed analyses of the prefactors in (A.8) and (A.12) show. Therefore, the leading $(\ln L)/(2L)$ correction for the surface tension is more generally valid; see also ref. 22. The finite-size behavior of the SOS and RSOS models is almost identical, except for differences in various nonuniversal coefficients and a notable change of the sign of the leading finite-size correction term b for the RSOS surface stiffness coefficient [see (4.14)]. The equivalence among the three models is recaptured in the low-temperature limit, as expected (see Appendix B).

APPENDIX A: EXACT PARTITION FUNCTIONS FOR THE SOLID-ON-SOLID MODELS

Our goal is to evaluate exactly the partition function

$$Z_{\mathrm{SOS}}(m, L) = \frac{v^{L+1}(1-u^2)^L}{2\pi} \int_{-\pi}^{\pi} \frac{\cos mq \, dq}{(1 - 2u \cos q + u^2)^L} \tag{A.1}$$

and it is instructive to describe the calculation in some detail. Consider the integral

$$I(m, L) = \int_{-\pi}^{\pi} \left(1 - \frac{2u \cos q}{1+u^2}\right)^{-L} \cos mq \, dq \tag{A.2}$$

This integral can be evaluated in the closed form by the use of tables[24] and certain algebraic manipulations. In particular, (A.2) can be expressed in terms of the associated Legendre functions $P^m_{L-1}(\cos\phi)$. First, introduce the auxiliary variable ϕ by

$$\frac{1+u^2}{2u} = \frac{i}{\tan\phi} \tag{A.3}$$

and use the integral representation[24]

$$P^m_{L-1}(x) = \frac{(-i)^m(L-1)!}{2\pi(L-m-1)!}\int_{-\pi}^{\pi} [x + i(1-x^2)^{1/2}\cos q]^{-L}\cos mq\, dq \tag{A.4}$$

After a little algebra we obtain

$$I(m, L) = \frac{2\pi(L-m-1)!}{(-i)^m(L-1)!}\cos^L(\phi)\, P^m_{L-1}(\cos\phi) \tag{A.5}$$

where the variable ϕ is defined by (A.3). The next step is to express the associated Legendre function $P^m_n(x)$ in terms of the hypergeometric function ${}_2F_1$ via[24]

$$P^m_n(x) = \frac{(-1)^m(2n)!}{2^{2n-m}n!\,(n-m)!}(1-x^2)^{m/2}[x+(x^2-1)^{1/2}]^{n-m} \times {}_2F_1\left(m-n, \frac{1}{2}+m, \frac{1}{2}-n, \frac{x-(x^2-1)^{1/2}}{x+(x^2-1)^{1/2}}\right) \tag{A.6}$$

Finally, we perform the Kummer transformation[24] on the hypergeometric function ${}_2F_1$, i.e.,

$${}_2F_1(\alpha, \beta, \gamma, z) = (1-z)^{-\beta}\, {}_2F_1\left(\beta, \gamma-\alpha, \gamma, \frac{z}{z-1}\right) \tag{A.7}$$

Note that, after transformations (A.6) and (A.7), the L dependence of P^m_{L-1} will be contained in the third parameter γ of the hypergeometric function, which is a power series in terms of $1/\gamma$. With the use of (A.5)–(A.7) and definition (A.3), after a long but straightforward algebra, the partition function (A.1) reduces to

$$Z_{\mathrm{SOS}}(m, L) = v^{L+1}\frac{\Gamma(L-\frac{1}{2})}{\Gamma(L)}\left(\frac{1+u}{1-u}\right)^L\left[\frac{1}{2\pi}\frac{(1-u)^2}{2u}\right]^{1/2} \times {}_2F_1\left(\frac{1}{2}+m, \frac{1}{2}-m, \frac{3}{2}-L, -\frac{(1-u)^2}{2u}\right) \tag{A.8}$$

where $\Gamma(x)$ is the usual gamma function. Note that the m dependence of $Z_{\mathrm{SOS}}(m, L)$ enters only in the function ${}_2F_1$ in a symmetric way, i.e., $Z(-m, L) = Z(m, L)$, as expected.

In a similar manner, the RSOS partition function

$$Z_{\mathrm{RSOS}}(m, L) = \frac{v^{L+1}}{2\pi} \int_{-\pi}^{\pi} (1 + 2u \cos q)^L \cos mq \, dq \tag{A.9}$$

can be evaluated exactly. First, we introduce the auxiliary variable ϕ by

$$2u = i \tan \phi \tag{A.10}$$

and recall[24] that

$$P_L^m(x) = \frac{i^m (L+m)!}{2\pi L!} \int_{-\pi}^{\pi} [x + i(1-x^2)^{1/2} \cos q]^L \cos mq \, dq \tag{A.11}$$

Second, we express P_L^m via (A.6) in terms of ${}_2F_1$ and, finally, transform ${}_2F_1$ by the use of (A.7). The final result, after a long algebra, is

$$Z_{\mathrm{RSOS}}(m, L) = v^{L+1} \binom{2L}{L-m} \left(\frac{1+2u}{4}\right)^L \left(\frac{1+2u}{4u}\right)^{1/2} \times {}_2F_1\left(\frac{1}{2}+m, \frac{1}{2}-m, \frac{1}{2}-L, \frac{2u-1}{4u}\right) \tag{A.12}$$

Note that this expression reduces to a very simple form for $u = 1/2$,

$$Z_{\mathrm{RSOS}}\left(m, L; u = \frac{1}{2}\right) = v \left(\frac{v}{2}\right)^L \binom{2L}{L-m} \tag{A.13}$$

which can, in fact, be used to study the pattern of *higher-order* finite-size corrections.

APPENDIX B: EQUIVALENCE BETWEEN ISING AND SOLID-ON-SOLID MODELS AT LOW TEMPERATURES

In this Appendix we show that the results obtained for the finite-size corrections of Ising and solid-on-solid models, (4.11)–(4.16), become identical at low temperatures. This can be achieved by identifying

$$U = 2K_x, \qquad V = 2K_y \tag{B.1}$$

in the SOS Hamiltonian (2.6), so that

$$u = \exp(-2K_x), \qquad v = \exp(-2K_y) \tag{B.2}$$

in (3.1), etc.

First, we report the results on finite-size corrections for the anisotropic ($K_x \neq K_y$) Ising model surface tension and stiffness coefficient τ_L and κ_L. This calculation has been outlined in Section 4 and we only quote the results here:

$$\tau = \gamma(0) \equiv 2(K_y - K_x^*), \qquad a = 2K_y \tag{B.3}$$

and

$$\kappa = \frac{\sinh \gamma(0)}{\sinh 2K_x^* \sinh 2K_y} \tag{B.4}$$

$$b = \frac{1}{2}\left[\frac{\sinh^2 \gamma(0)}{\sinh^2 2K_x^* \sinh^2 2K_y} + \frac{3\cosh \gamma(0)}{\sinh 2K_x^* \sinh 2K_y} + \frac{1}{\sinh^2 2K_y}\right] \tag{B.5}$$

Derivation of (B.5) requires rather long algebraic calculations.

In the low-temperature limit $K_y \equiv J_y/k_B T$ is large, while K_x^* is exponentially small. We thus obtain the leading results

$$\tau \simeq 2K_y, \qquad a = 2K_y, \qquad \kappa \simeq e^{2K_x}/2, \qquad b \simeq e^{4K_x}/8 \tag{B.6}$$

On the other hand, the SOS model results (4.11)–(4.14) in the low-temperature limit (u, v small) give

$$\tau \simeq -\ln v, \qquad a = -\ln v, \qquad \kappa \simeq \frac{1}{2u}, \qquad b \simeq \frac{1}{8u^2} \tag{B.7}$$

By (B.2), the results (B.6) and (B.7) are identical, as anticipated. As shown in ref. 25, the unrestricted SOS model calculation of the surface tension τ (but not κ) reproduces, in fact, the *exact* 2D Ising model result. Indeed,

$$\begin{aligned} \gamma(0) &\equiv 2(K_y - K_x^*) = \ln(e^{2K_y} e^{-2K_x^*}) \\ &= \ln(e^{2K_y} \tanh K_x) = -\ln\left(v\frac{1+u}{1-u}\right) \end{aligned} \tag{B.8}$$

It is interesting that the SOS model result for the leading $1/L$ correction coefficient a is also exact [see (4.12) and (2.15)–(2.17)].

ACKNOWLEDGMENTS

Research by V.P. and N.M.S. has been supported in part by the U.S. National Science Foundation under grant DMR-86-01208, and by the donors of the Petroleum Research Fund, administered by the American Chemical Society, under grant ACS-PRF-18175-G6. This financial assistance is gratefully acknowledged.

REFERENCES

1. M. E. Fisher, in *Critical Phenomena*, M. S. Green, ed. (Academic Press, New York, 1971), p. 1.
2. M. N. Barber, in *Phase Transitions and Critical Phenomena*, Vol. 8, C. Domb and J. L. Lebowitz, eds. (Academic Press, New York, 1983), p. 145.
3. V. Privman and M. E. Fisher, *J. Stat. Phys.* **33**:385 (1983).
4. K. Binder and D. P. Landau, *Phys. Rev. B* **30**:1477 (1984).
5. M. E. Fisher and V. Privman, *Phys. Rev. B* **32**:447 (1985).
6. M. S. S. Challa, D. P. Landau, and K. Binder, *Phys. Rev. B* **34**:1836 (1986).
7. D. Sullivan and M. M. Telo da Gama, in *Fluid and Interfacial Phenomena*, C. A. Croxton, ed. (Wiley, New York, 1986).
8. H. Nakanishi and M. E. Fisher, *J. Chem. Phys.* **78**:3279 (1983).
9. H. Au-Yang and M. E. Fisher, *Phys. Rev. B* **21**:3956 (1980).
10. D. B. Abraham, in *Phase Transitions and Critical Phenomena*, Vol. 10, C. Domb and J. L. Lebowitz, eds. (Academic Press, New York, 1986), p. 1.
11. D. B. Abraham and N. M. Švrakić, *Phys. Rev. Lett.* **56**:1172 (1986).
12. G. Forgacs, N. M. Švrakić, and V. Privman, *Phys. Rev. B* **37**:3818 (1988).
13. V. Privman and N. M. Švrakić, *Phys. Rev. B* **37**:3713 (1988).
14. R. Lipowsky and G. Gompper, *Phys. Rev. B* **29**:5213 (1984).
15. T. W. Burkhardt and I. Guim, *Phys. Rev. B* **35**:1799 (1987).
16. K. K. Mon, S. Wansleben, D. P. Landau, and K. Binder, *Phys. Rev. Lett.* **60**:708 (1988).
17. V. Privman, *Phys. Rev. Lett.* **61**:183 (1988).
18. M. P. Gelfand and M. E. Fisher, *Int. J. Thermophys.* (1988), in press.
19. M. E. Fisher, *J. Stat. Phys.* **34**:667 (1984).
20. D. S. Fisher and J. D. Weeks, *Phys. Rev. Lett.* **50**:1077 (1983).
21. R. F. Kayser, *Phys. Rev. A* **33**:1948 (1986).
22. H. Park, E. K. Riedel, and M. den Nijs, *Ann. Phys.* (N.Y.) **172**:419 (1986).
23. D. B. Abraham, *Stud. Appl. Math.* **50**:71 (1971).
24. I. S. Gradshteyn and I. M. Ryzhik, *Table of Integrals, Series, and Products* (Academic Press, New York, 1980).
25. E. Müller-Hartmann and J. Zittartz, *Z. Phys. B* **27**:261 (1977).